

# Liquidus phase relationships on the join anorthite-forsterite-quartz at 20 kbar with applications to basalt petrogenesis and igneous sapphirine\*

Teh-Ching Liu and Dean C. Presnall

Geosciences Program, The University of Texas at Dallas, P.O. Box 830688, Richardson, TX 75083-0688, USA

Received June 17, 1988 / Accepted January 7, 1990

**Abstract.** Liquidus phase relationships determined on the join anorthite-forsterite-quartz at 20 kbar show primary phase fields for quartz (*q*), forsterite (*fo*), enstatite (*en*), spinel (*sp*), anorthite (*an*), sapphirine (*sa*), and corundum (*cor*). Increasing pressure causes (1) the *fo* and *an* primary phase fields to contract, (2) the *en*, *q*, and *cor* fields to expand, (3) the *fo-en* boundary line to move away from the Q apex, (4) the *en-q* boundary line to move also away from the Q apex but by a smaller amount, and (5) a primary phase field for *sa* to appear at a pressure between 10 and 20 kbar. Seven liquidus piercing points at 20 kbar have been located as follows:

Crystalline phases	Liquid composition (wt %)	Temperature (° C)
<i>sp</i> + <i>sa</i> + <i>cor</i>	An <sub>81</sub> Fo <sub>17</sub> Q <sub>2</sub>	1575
<i>fo</i> + <i>en</i> + <i>sp</i>	An <sub>52</sub> Fo <sub>39</sub> Q <sub>9</sub>	1540
<i>en</i> + <i>sp</i> + <i>sa</i>	An <sub>59</sub> Fo <sub>31</sub> Q <sub>10</sub>	1490
<i>sa</i> + <i>an</i> + <i>cor</i>	An <sub>70</sub> Fo <sub>15</sub> Q <sub>15</sub>	1430
<i>an</i> + <i>q</i> + <i>cor</i>	An <sub>66</sub> Fo <sub>7</sub> Q <sub>27</sub>	1410
<i>sa</i> + <i>an</i> + <i>en</i>	An <sub>62</sub> Fo <sub>18</sub> Q <sub>20</sub>	1400
<i>an</i> + <i>en</i> + <i>q</i>	An <sub>59</sub> Fo <sub>15</sub> Q <sub>26</sub>	1380

It is concluded that (1) the shift of the *fo-en* boundary line away from the quartz apex with pressure confirms many other studies showing that melts generated from peridotite source rocks decrease in silica content as pressure increases; (2) even though plagioclase is not a stable phase in peridotite source rocks at pressures above about 10 kbar, it can crystallize from mafic magmas at pressures at least up to 20 kbar; (3) sapphirine crystallizes from mafic magmas at high pressures and may be important in the construction of petrogenetic models based on trace element considerations.

## Introduction

Phase relationships in the system CaO–MgO–Al<sub>2</sub>O<sub>3</sub>–SiO<sub>2</sub> (CMAS) (Fig. 1) have been used extensively to

model the generation of basaltic magmas from a peridotite or eclogite source and the crystallization of these magmas at various pressure (O'Hara 1965, 1968; O'Hara and Yoder 1967; Presnall et al. 1978, 1979). Nevertheless, the known phase relationships in this system remain very limited. For tholeiitic magma, the most important part of this system is the tetrahedron forsterite-diopside-anorthite-quartz that serves as a simplified version of the tholeiitic portion of the basalt tetrahedron of Yoder and Tilley (1962).

This study is a determination of liquidus phase relationships at 20 kbar on the forsterite-anorthite-quartz base of the simplified tholeiitic basalt tetrahedron. Previous studies of the join forsterite-anorthite-quartz have been carried out at atmospheric pressure (Andersen 1915; Irvine 1975; Longhi 1987) and at 10 kbar (Sen

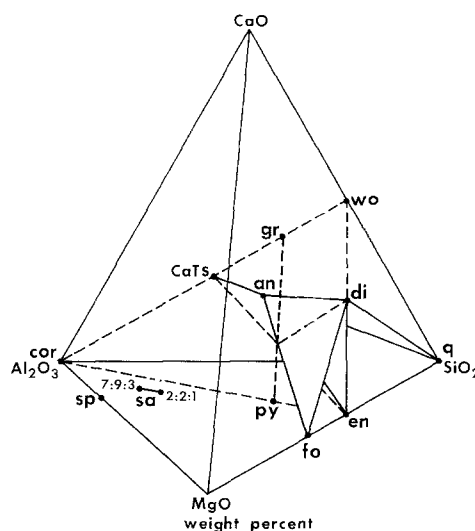


**Fig. 1.** The system CaO–MgO–Al<sub>2</sub>O<sub>3</sub>–SiO<sub>2</sub> with the simplified tholeiitic basalt tetrahedron fo-di-an-q. All dashed lines lie in the join Al<sub>2</sub>O<sub>3</sub>–en–wo. *wo*, wollastonite (CaSiO<sub>3</sub>); *gr*, grossularite (Ca<sub>3</sub>Al<sub>2</sub>Si<sub>3</sub>O<sub>12</sub>); *CaTs*, Ca Tschermak's molecule (CaAl<sub>2</sub>SiO<sub>6</sub>); *cor*, corundum (Al<sub>2</sub>O<sub>3</sub>); *sp*, spinel (MgAl<sub>2</sub>O<sub>4</sub>); *sa*, sapphirine (MgO:Al<sub>2</sub>O<sub>3</sub>:SiO<sub>2</sub> ratios shown); *an*, anorthite (CaAl<sub>2</sub>Si<sub>2</sub>O<sub>8</sub>); *di*, diopside (CaMgSi<sub>2</sub>O<sub>6</sub>); *py*, pyrope (Mg<sub>3</sub>Al<sub>2</sub>Si<sub>3</sub>O<sub>12</sub>); *fo*, forsterite (Mg<sub>2</sub>SiO<sub>4</sub>); *en*, enstatite (MgSiO<sub>3</sub>); *q*, quartz (SiO<sub>2</sub>)

\* Contribution No. 588, Geosciences Program, The University of Texas at Dallas

Offprint requests to: D.C. Presnall

and Presnall 1984). Most of the liquidus phase relationships on this join at 20 kbar are not ternary and crystallization paths cannot be understood without reference to quaternary relationships in the CMAS tetrahedron. Nevertheless, this join is important as a limiting boundary for understanding quaternary phase relationships in the tetrahedron forsterite-diopside-anorthite-quartz. The phase relationships also show the surprising importance of sapphirine as a phase that crystallizes from basaltic liquids at high pressures.

### Experimental method

The glass starting mixtures used in this study are those used by Chen and Presnall (1975), Presnall et al. (1978), and Sen and Presnall (1984), and new mixtures prepared according to the procedures described by Presnall (1966) and Presnall et al. (1972). Experimental runs were carried out in a piston-cylinder apparatus (Boyd and England 1960). The pressure-cell assembly is the same as that described by Presnall et al. (1973), except that pyrex glass sleeves were used instead of boron nitride sleeves. Platinum capsules were used as sample containers. All assembly parts, except for the talc and glass sleeves, were dried for 45 min at 1050° C to keep the charges free of water. The glass sleeves were stored in an oven at 110° C.

All experiments were of the piston-out type (Presnall et al. 1978) with no pressure correction. In all cases, W3Re/W25Re thermocouples were used with no pressure correction applied to the emf values. Temperatures are corrected to the International Practical Temperature Scale of 1968 (Anonymous 1969).

A polished section of each run was made in the long (vertical) dimension of the capsule and examined in reflected light. Characteristic relief, reflectivity, and crystal habit were used for phase identification, along with electron microprobe analysis and back-scattered electron imaging in questionable cases.

The compositions of enstatite, sapphirine, and glass were determined with a JEOL model JXA-733 electron microprobe at Southern Methodist University. Their standard WIGLI-22 (a synthetic glass) was used for the analysis of Si and Ca. A synthetic spinel, MGALS-52, was used as a standard for the analysis of Al and Mg. Grains of enstatite and sapphirine chosen for analysis are usually larger than 10 µm in diameter and the diameter of analyzed glass pools is usually larger than 30 µm. Microprobe operating conditions were 15 kV accelerating potential, 0.02 microamperes beam current and 1 µm beam diameter. The wavelength-dispersive method was used in all chemical analyses, and all data were corrected by the Bence-Albee procedure with the alpha factors of Albee and Ray (1970).

Analyses were accepted if they had sums between 99 and 101 wt %. An additional criterion for the acceptance of enstatite analyses was a structural formula showing between 3.96 and 4.04 cations per six oxygen atoms.

### Reversal experiments

Reversal experiments were used to determine run durations necessary for chemical equilibrium. Following the procedure of Presnall et al. (1978), a liquidus bracket for each of the primary phase fields has been reversed (except for corundum, due to problems listed in Presnall et al. 1978). Within a given primary phase field, it is assumed that other unreversed experiments extending for a time as long or longer than the reversal experiments

**Table 1.** Reversal experiments

Run no.	Initial condition		Final condition		Phases <sup>a</sup>
	Temperature (° C)	Duration (h)	Temperature (° C)	Duration (h)	
40% CaAl <sub>2</sub> Si <sub>2</sub> O <sub>8</sub> , 60% MgSiO <sub>3</sub> <sup>b</sup>					
391-5	1540	5	1600	5	gl
391-6	1600	5	1540	5	gl+en
80% CaAl <sub>2</sub> Si <sub>2</sub> O <sub>8</sub> , 20% Mg <sub>2</sub> SiO <sub>4</sub>					
378-5	1590	5	1650	4	gl
378-6	1650	4	1590	5	gl+sp
50% CaAl <sub>2</sub> Si <sub>2</sub> O <sub>8</sub> , 42% Mg <sub>2</sub> SiO <sub>4</sub> , 8% SiO <sub>2</sub> (AFQ-22)					
378-15	1540	6	1600	4	gl
378-1	1600	4	1540	6	gl+fo
54% CaAl <sub>2</sub> Si <sub>2</sub> O <sub>8</sub> , 15% Mg <sub>2</sub> SiO <sub>4</sub> , 31% SiO <sub>2</sub> (GS-3)					
377-12	1490	24	1550	24	gl
373-12	1550	24	1490	24	gl+q
60% CaAl <sub>2</sub> Si <sub>2</sub> O <sub>8</sub> , 23% Mg <sub>2</sub> SiO <sub>4</sub> , 17% SiO <sub>2</sub> (GS-2)					
375-6	1420	8	1480	8	gl
375-9	1480	8	1420	8	gl+en
67% CaAl <sub>2</sub> Si <sub>2</sub> O <sub>8</sub> , 17% Mg <sub>2</sub> SiO <sub>4</sub> , 16% SiO <sub>2</sub> (GS-5)					
391-7	1410	6	1470	6	gl
391-8	1470	6	1410	6	gl+sa
68% CaAl <sub>2</sub> Si <sub>2</sub> O <sub>8</sub> , 13% Mg <sub>2</sub> SiO <sub>4</sub> , 19% SiO <sub>2</sub> (AFQ-24)					
388-2	1390	23	1450	6	gl
383-1	1450	6	1390	23	gl+an

<sup>a</sup> *an*, anorthite; *cor*, corundum; *en*, enstatite; *fo*, forsterite; *gl*, glass; *q*, quartz; *sa*, sapphirine; *sp*, spinel

<sup>b</sup> Proportion in wt%

represent equilibrium results. The number of hours required for equilibrium are 5 for spinel at 1590° C, 6 for forsterite at 1540° C, 5 for enstatite at 1540° C, 8 for enstatite at 1420° C, 6 for sapphirine at 1410° C, 23 for anorthite at 1390° C, and 24 for quartz at 1490° C (Table 1). For runs at higher temperatures, run durations are based on previous reversal runs given by Chen and Presnall (1975), Presnall (1976), Presnall et al. (1978), and Sen and Presnall (1984).

### Data

The liquidus surface of the join An-Fo-Q at 20 kbar, shown in Fig. 2, is based on quenching experiments and glass analyses given, respectively, in Tables 2 and 3. Our data agree mostly but not entirely with previous data on this join at 20 kbar. Mixture A (Fo<sub>76</sub>Q<sub>24</sub>)<sup>1</sup> of Chen and Presnall (1975) was re-studied here. The present data (Table 2) are consistent with those of Chen and Presnall (1975) when temperature uncertainties of ±10° C are taken into account. However, our present data added to the earlier data of Chen and Presnall (1975) indicate

<sup>1</sup> This and subsequent compositions are given in weight percent

**Table 2.** Quenching experiments

Run no.	Temp. (° C)	Duration (h)	Phases <sup>a</sup>	Run no.	Temp. (° C)	Duration (h)	Phases <sup>a</sup>
76% Mg <sub>2</sub> SiO <sub>4</sub> , 24% SiO <sub>2</sub> (A) <sup>b</sup>				60% CaAl <sub>2</sub> Si <sub>2</sub> O <sub>8</sub> , 12% Mg <sub>2</sub> SiO <sub>4</sub> , 28% SiO <sub>2</sub> (GS-6)			
389-1	1770	1	gl	377-13	1450	24	gl
390-1	1760	1	gl+fo+en+(px)+(fo)	371-6	1430	51	gl+q
20% CaAl <sub>2</sub> Si <sub>2</sub> O <sub>8</sub> , 80% MgSiO <sub>3</sub>				371-7	1390	24	gl+q
374-10	1690	1.75	gl	375-12	1370	24	gl+q+an
374-11	1670	4	gl+en+(px)	378-12	1360	24	gl+q+an+en
40% CaAl <sub>2</sub> Si <sub>2</sub> O <sub>8</sub> , 60% MgSiO <sub>3</sub>				375-13	1350	26	q+an+en
374-8	1580	4	gl	62% CaAl <sub>2</sub> Si <sub>2</sub> O <sub>8</sub> , 22% Mg <sub>2</sub> SiO <sub>4</sub> , 16% SiO <sub>2</sub> (GS-8)			
374-9	1560	4	gl+en+(px)	371-8	1450	8	gl
60% CaAl <sub>2</sub> Si <sub>2</sub> O <sub>8</sub> , 40% MgSiO <sub>3</sub>				375-14	1440	16	gl+sa
372-6	1500	8	gl	371-9	1430	16	gl+sa+en
372-8	1480	8	gl+sa+en	371-10	1410	8	gl+sa+en
80% CaAl <sub>2</sub> Si <sub>2</sub> O <sub>8</sub> , 20% MgSiO <sub>3</sub>				378-13	1390	24	gl+sa+en+an
377-10	1570	6	gl	375-15	1350	50	en+an+q
372-5	1550	6	gl+cor	64% CaAl <sub>2</sub> Si <sub>2</sub> O <sub>8</sub> , 23% Mg <sub>2</sub> SiO <sub>4</sub> , 13% SiO <sub>2</sub> (GS-11)			
45% CaAl <sub>2</sub> Si <sub>2</sub> O <sub>8</sub> , 55% Mg <sub>2</sub> SiO <sub>4</sub>				374-1	1480	5.5	gl
377-4	1705	4	gl+(fo)	374-2	1450	6	gl+sa
377-5	1685	4	gl+fo+(fo)	65% CaAl <sub>2</sub> Si <sub>2</sub> O <sub>8</sub> , 8% Mg <sub>2</sub> SiO <sub>4</sub> , 27% SiO <sub>2</sub> (AFQ-23)			
377-6	1665	4	gl+fo+sp+(fo)	378-19	1420	24	gl
380-1	1625	4	gl+fo+sp+(fo)	378-3	1400	24	gl+q+an
380-2	1585	4	gl+fo+sp+(fo)	379-1	1380	24	gl+q+an
80% CaAl <sub>2</sub> Si <sub>2</sub> O <sub>8</sub> , 20% Mg <sub>2</sub> SiO <sub>4</sub>				379-2	1360	24	gl+q+an+en
377-2	1630	5	gl	67% CaAl <sub>2</sub> Si <sub>2</sub> O <sub>8</sub> , 17% Mg <sub>2</sub> SiO <sub>4</sub> , 16% SiO <sub>2</sub> (GS-5)			
372-3	1610	5	gl+sp	371-1	1450	8	gl
45% CaAl <sub>2</sub> Si <sub>2</sub> O <sub>8</sub> , 42% Mg <sub>2</sub> SiO <sub>4</sub> , 13% SiO <sub>2</sub> (GS-1)				371-2	1430	10	gl+sa
373-5	1560	8	gl	378-10	1390	24	gl+sa+an
373-6	1550	6	gl+en+(px)	378-11	1370	25	gl+an+en
375-5	1480	51	gl+en+(px)	68% CaAl <sub>2</sub> Si <sub>2</sub> O <sub>8</sub> , 13% Mg <sub>2</sub> SiO <sub>4</sub> , 19% SiO <sub>2</sub> (AFQ-24)			
50% CaAl <sub>2</sub> Si <sub>2</sub> O <sub>8</sub> , 42% Mg <sub>2</sub> SiO <sub>4</sub> , 8% SiO <sub>2</sub> (AFQ-22)				378-4	1430	10	gl
377-15	1580	4	gl	379-4	1410	25	gl+an
377-16	1560	5	gl+fo	379-5	1390	25	gl+an
53% CaAl <sub>2</sub> Si <sub>2</sub> O <sub>8</sub> , 38% Mg <sub>2</sub> SiO <sub>4</sub> , 9% SiO <sub>2</sub> (AFQ-21)				379-6	1370	24	gl+an+en
376-3	1520	8	gl	70% CaAl <sub>2</sub> Si <sub>2</sub> O <sub>8</sub> , 4% Mg <sub>2</sub> SiO <sub>4</sub> , 26% SiO <sub>2</sub> (AFQ-26)			
376-9	1510	8	gl+en+sp+(px)	380-13	1490	18	gl
54% CaAl <sub>2</sub> Si <sub>2</sub> O <sub>8</sub> , 15% Mg <sub>2</sub> SiO <sub>4</sub> , 31% SiO <sub>2</sub> (GS-3)				380-14	1470	24	gl+cor
373-10	1530	24	gl	72% CaAl <sub>2</sub> Si <sub>2</sub> O <sub>8</sub> , 14% Mg <sub>2</sub> SiO <sub>4</sub> , 14% SiO <sub>2</sub> (AFQ-28)			
373-11	1510	24	gl+q	381-6	1460	6	gl
373-15	1400	24	gl+q	381-7	1440	6	gl+cor
373-16	1360	24	gl+q+en	72% CaAl <sub>2</sub> Si <sub>2</sub> O <sub>8</sub> , 19% Mg <sub>2</sub> SiO <sub>4</sub> , 9% SiO <sub>2</sub> (AFQ-25)			
55% CaAl <sub>2</sub> Si <sub>2</sub> O <sub>8</sub> , 35% Mg <sub>2</sub> SiO <sub>4</sub> , 10% SiO <sub>2</sub> (GS-0)				380-11	1510	8	gl
372-9	1530	5	gl	379-8	1490	8	gl+sa
372-10	1520	8	gl+en+sp+(px)	55% CaAl <sub>2</sub> Si <sub>2</sub> O <sub>8</sub> , 20% Mg <sub>2</sub> SiO <sub>4</sub> , 25% SiO <sub>2</sub> (AFQ-20)			
375-18	1430	8	gl	375-18	1430	8	gl
376-6	1410	24	gl+en	376-6	1410	24	gl+en
376-1	1390	24	gl+en	376-1	1390	24	gl+en
380-6	1370	24	gl+en+q+an	380-6	1370	24	gl+en+q+an
60% CaAl <sub>2</sub> Si <sub>2</sub> O <sub>8</sub> , 23% Mg <sub>2</sub> SiO <sub>4</sub> , 17% SiO <sub>2</sub> (GS-2)				375-8	1460	8	gl
375-8	1460	8	gl	373-8	1440	16	gl+en
373-8	1440	16	gl+en	375-10	1380	24	gl+en+an
375-10	1380	24	gl+en+an				

<sup>a</sup> Abbreviations same as in Table 1. Parentheses indicate phases formed during quenching

<sup>b</sup> Proportions in wt%

that the forsterite-enstatite eutectic is located at the composition of mixture A (76% Mg<sub>2</sub>SiO<sub>4</sub>, 24% SiO<sub>2</sub>) at about 23 kbar, 1780° C. This location is about 4 kbar and 20° C lower than that extrapolated by Chen and Presnall (1975). Therefore, at any given pressure, the fo-en eutectic is displaced slightly toward Fo from the location given by Chen and Presnall (1975).

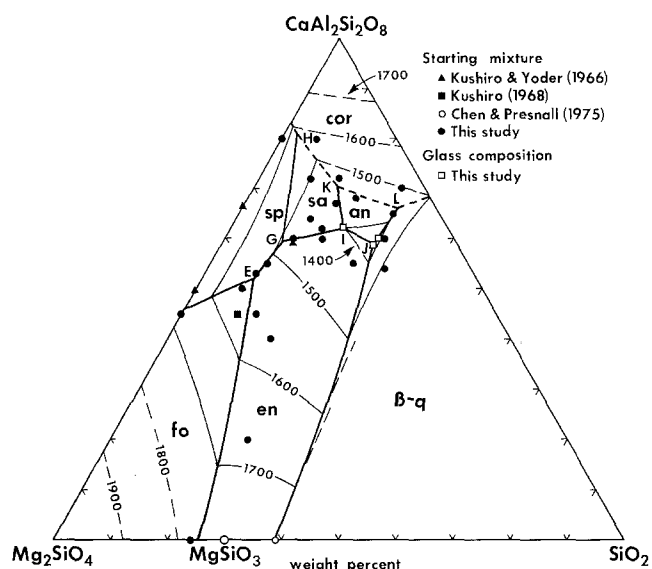


**Fig. 2.** Liquidus surface of the join  $\text{CaAl}_2\text{Si}_2\text{O}_8$ – $\text{Mg}_2\text{SiO}_4$ – $\text{SiO}_2$  at 20 kbar. Data on the bounding binary system  $\text{Mg}_2\text{SiO}_4$ – $\text{SiO}_2$  and on the bounding joins  $\text{CaAl}_2\text{Si}_2\text{O}_8$ – $\text{SiO}_2$  and  $\text{Mg}_2\text{SiO}_4$ – $\text{CaAl}_2\text{Si}_2\text{O}_8$  are from Chen and Presnall (1975), Clark et al. (1962), and Presnall et al. (1978), respectively. Liquidus temperatures from Chen and Presnall (1975) and Presnall et al. (1978) have been raised 20° C (see discussion in Sen and Presnall 1984, p 405). The position of the fo-en eutectic given by Chen and Presnall (1975) has been revised (see text)

**Table 3.** Glass compositions (wt%)

Mixture No.	GS–8	AFQ–20	AFQ–23
Run no.	378–13	380–6	379–1
No. of spots	6	6	3
$\text{SiO}_2$	53.91 (0.15) <sup>a</sup>	58.07 (0.08)	58.33 (0.21)
$\text{Al}_2\text{O}_3$	22.52 (0.11)	21.36 (0.07)	22.08 (0.12)
MgO	10.48 (0.04)	8.48 (0.04)	7.47 (0.04)
CaO	12.52 (0.20)	11.97 (0.22)	12.05 (0.16)
Sum	99.43	99.88	99.93
$\text{CaMgSi}_2\text{O}_6$	0.51	0.85	–0.36
$\text{CaAl}_2\text{Si}_2\text{O}_8$	61.80	58.35	60.29
$\text{Mg}_2\text{SiO}_4$	18.23	14.54	13.16
$\text{SiO}_2$	19.45	26.25	26.90

<sup>a</sup> Standard error of the mean in parentheses

For the mixture  $\text{An}_{66.4}\text{Fo}_{33.6}$  at 20 kbar, Kushiro and Yoder (1966) found spinel to be the primary phase at a liquidus temperature of 1693° C. Kushiro (1968) studied the mixture  $\text{An}_{45}\text{Fo}_{45}\text{Q}_{10}$  (DP–65) and found the liquidus temperature to be 1580° C and the primary phase to be forsterite. Both of these results are consistent with our data, as shown in Fig. 2. Another composition studied by Kushiro and Yoder (1966),  $\text{An}_{59}\text{En}_{41}$ , is close to the piercing point,  $sp+sa+en+liq$ , in Fig. 2. They estimated this composition to have a liquidus temperature higher than 1550° C, with spinel as the liquidus phase. We have determined the liquidus temperature of the mixture,  $\text{An}_{60}\text{En}_{40}$ , to be 1490° C, and the liquidus

**Table 4.** Compositions of piercing points (wt%)

Point	Temperature (° C)	$\text{CaAl}_2\text{Si}_2\text{O}_8$	$\text{Mg}_2\text{SiO}_4$	$\text{SiO}_2$
E	1540	52.0	39.2	8.8
G	1490	59.3	30.5	10.2
H	1575	80.7	17.0	2.3
I	1400	62.0	18.4	19.6
J	1370	58.7	14.8	26.5
K	1430	70.4	15.2	14.4
L	1410	66.1	6.8	27.1

phases are enstatite and sapphirine. The reason for this discrepancy is unknown.

Mixtures  $\text{An}_{80}\text{Fo}_{20}$  and  $\text{An}_{45}\text{Fo}_{55}$  were studied by Presnall et al. (1978) and re-studied here. Our liquidus temperatures for these mixtures are 15 and 40° C higher, respectively, than those of Presnall et al. (1978). This difference is due to the fact that Presnall et al. (1978) used boron nitride sleeves in the high pressure assembly rather than pyrex, as used here. Boron nitride apparently allows a small amount of  $\text{H}_2$  to diffuse into the capsule. The  $\text{H}_2$  then reacts with oxygen in the sample to form water, which slightly reduces the liquidus temperature. Charge balance in the sample is maintained by diffusion of Si from the sample into the Pt capsule to form a Pt–Si alloy (Chen and Presnall 1975). Although the liquidus temperatures determined by Presnall et al. (1978) are slightly low, the positions of boundary lines determined by them are consistent with our results.

On the  $\text{SiO}_2$ – $\text{CaAl}_2\text{Si}_2\text{O}_8$  boundary, Clark et al. (1962) found a liquidus boundary between quartz and sillimanite at 66.3%  $\text{CaAl}_2\text{Si}_2\text{O}_8$  and a second boundary between sillimanite and corundum located at some undefined position closer to  $\text{CaAl}_2\text{Si}_2\text{O}_8$ . We have no new data on the join  $\text{SiO}_2$ – $\text{CaAl}_2\text{Si}_2\text{O}_8$  but no sillimanite has been found in any of our experiments on mixtures close to this join. Figure 2 has been drawn without a primary phase field for sillimanite and with a boundary between beta-quartz and corundum located on the join  $\text{SiO}_2$ – $\text{CaAl}_2\text{Si}_2\text{O}_8$  at 68%  $\text{CaAl}_2\text{Si}_2\text{O}_8$ . This position fits our ternary data best, but the possibility still exists for a small sillimanite field between the beta-quartz and corundum fields along the join  $\text{SiO}_2$ – $\text{CaAl}_2\text{Si}_2\text{O}_8$ .

Compositions of seven piercing points found within the join An–Fo–Q (Fig. 2) are listed in Table 4. All of these piercing points except I and J were located by the classical procedure of bracketing them between liquidus primary phase determinations for nearby bulk compositions. Points I and J (Table 3, columns 1 and 2) and the compositions of enstatite (Table 5) in equilibrium with the liquids at I and J were determined by electron microprobe analysis. The analyzed glasses have compositions that lie only slightly off the plane of the diagram toward diopside (0.51% and 0.85% normative diopside, respectively). Because of the very small amounts of excess diopside, which only marginally exceed the analytical uncertainty, these compositions have been projected from diopside onto the join An–Fo–Q and used as the piercing point liquid compositions.

**Table 5.** Enstatite compositions (wt%)

Mix. No.	GS-8	AFQ-20
Run No.	378-13	380-6
No. of spots	2	4
SiO <sub>2</sub>	52.66	53.09 (0.19) <sup>a</sup>
Al <sub>2</sub> O <sub>3</sub>	12.71	11.77 (0.21)
MgO	32.70	33.49 (0.22)
CaO	1.94	1.91 (0.09)
Sum	100.01	100.26
Number of cations for 6 oxygens		
Si	1.768	1.780
Al <sup>IV</sup>	0.232	0.220
Al <sup>VI</sup>	0.270	0.244
Mg	1.636	1.673
Ca	0.069	0.068
Sum	3.975	3.985

<sup>a</sup> Standard error of the mean in parentheses

On the assumption that anorthite does not contain Mg, anorthite and beta-quartz are the only crystalline phases that lie on the plane of the diagram. Therefore, the only ternary boundary line is the one between anorthite and beta-quartz. All other boundaries are intersections of quaternary divariant surfaces with the plane of the diagram. The beta-quartz-anorthite boundary has been located at one point (Fig. 2) by electron microprobe analysis of the glass in run 379-1 (Table 3, column 3). Because the boundary line is ternary, the glass composition must lie on the plane of the diagram. The deviation from this plane (shown in Table 3 as -0.36% normative diopside) is within the analytical uncertainty.

Boundary lines limiting the corundum primary phase field and liquidus isotherms within this field are dashed because reversals involving corundum could not be obtained in a reasonable amount of time (see Presnall et al. 1978). The data for this field (Table 2) are all internally consistent and possibly represent equilibrium results, but in the absence of reversals, these runs must be considered to represent synthesis data only.

In Fig. 3, the liquidus phase boundaries at 20 kbar are compared with those at atmospheric pressure (Andersen 1915; Irvine 1975) and at 10 kbar (Sen and Presnall 1984). The composition of the forsterite-enstatite eutectic shown by Sen and Presnall (1984) at 10 kbar was based on the earlier work of Chen and Presnall (1975). However, the position of this eutectic was not tightly constrained by Chen and Presnall. On the basis of our revised location for this eutectic at 20 kbar and a linear interpolation between atmospheric pressure and 20 kbar, we have moved the 10 kbar eutectic shown by Sen and Presnall (1984) slightly toward the SiO<sub>2</sub> apex.

Also, we have revised the enstatite-anorthite boundary determined by Sen and Presnall (1984) at 10 kbar. Mixture An<sub>54</sub> Fo<sub>15</sub> Q<sub>31</sub> studied by Sen and Presnall was incorrectly given in their Tables 1 and 2 as An<sub>52</sub> Fo<sub>15</sub> Q<sub>33</sub> and incorrectly plotted in their Fig. 1. Also, we have determined the liquidus temperature and primary phases

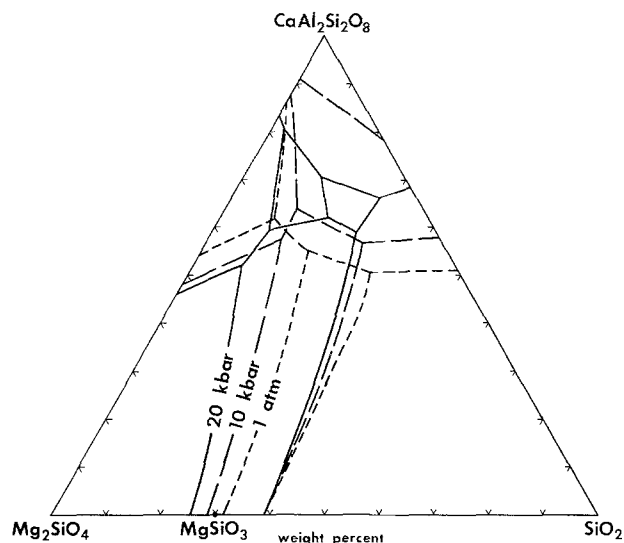


**Fig. 3.** Comparison of liquidus phase boundaries at 20 kbar with those at atmospheric pressure (Andersen 1915, as modified by Irvine 1975) and at 10 kbar (Sen and Presnall 1984). See text for discussion of adjustments to the boundary lines of Sen and Presnall (1984)

of mixture GS-8 (An<sub>62</sub> Fo<sub>22</sub> Q<sub>16</sub>) to be 1360° C and anorthite+enstatite at 10 kbar. This result is based on a run at 1370° C for 10 h that showed only glass and a run at 1350° C for 12.5 h that showed glass+anorthite+enstatite. On the basis of this new information, we have relocated the enstatite-anorthite-quartz piercing point at 10 kbar slightly toward the CaAl<sub>2</sub>Si<sub>2</sub>O<sub>8</sub> apex from its position shown by Sen and Presnall (compare Fig. 3 with their Fig. 1).

As has been found in earlier studies on similar joins, increasing pressure causes the forsterite and anorthite fields to shrink and the corundum, enstatite, and quartz fields to expand. A major difference in the phase relationships between 10 and 20 kbar is the presence of a sapphirine field at 20 kbar. In the system MgO-Al<sub>2</sub>O<sub>3</sub>-SiO<sub>2</sub>, Foster (1950a, 1950b) and Keith and Schairer (1952) found a primary phase field for sapphirine at atmospheric pressure. In the same system at 15 kbar, Taylor (1973) found that the primary phase field of sapphirine is noticeably larger, which is generally consistent with our results. On the basis of a study of the stability field of sapphirine in the system MgO-Al<sub>2</sub>O<sub>3</sub>-SiO<sub>2</sub>-H<sub>2</sub>O, Ackermann et al. (1975) concluded that 20 kbar and 30 kbar are, respectively, the upper limits for the formation of sapphirine under anhydrous conditions in shield regions and hydrous conditions in oceanic regions. The results of our study indicate that the stability of sapphirine at liquidus temperatures extends to pressures greater than 20 kbar under anhydrous conditions.

### Generation and crystallization of basaltic magma

As has been shown in numerous other studies (e.g.-O'Hara 1965, 1968; Green and Ringwood 1967; Kushiro

1968; Chen and Presnall 1975; Presnall et al. 1978, 1979; Stolper 1980; Sen and Presnall 1984), the boundary line between olivine and enstatite shifts away from the quartz apex as pressure increases. Therefore, primary magmas derived from a peridotite mantle would, under anhydrous or nearly anhydrous conditions, be progressively more depleted in silica with increasing pressure.

Because all the liquidus relationships except the quartz and anorthite primary phase fields are quaternary, crystallization paths cannot be described without reference to the tetrahedron in which the forsterite-anorthite-quartz plane lies. Nevertheless, two important features relevant to crystallization processes of basaltic magmas are shown by Fig. 2. One is the occurrence of sapphirine at the liquidus, which shows that sapphirine is a phase that would be expected to crystallize from basaltic magmas at high pressure and must be taken into account when fractional crystallization of basalts at high pressures is considered.

The second feature is the existence of anorthite at the liquidus. Anorthite stability at liquidus temperatures decreases as pressure increases, and the maximum stability of plagioclase peridotite in the CMAS system is 9 kbar (Presnall et al. 1979). However, Fig. 2 shows that for liquids higher in the  $\text{SiO}_2$  and  $\text{CaAl}_2\text{Si}_2\text{O}_8$  components than peridotite, anorthite remains a phase that crystallizes from mafic melts at pressures at least as high as 20 kbar.

### Igneous sapphirine

Sapphirine is generally considered to be of metamorphic origin (see review by Meng and Moore 1972), and has been found in high-grade regionally metamorphosed rocks (Dallwitz 1968; Morse and Talley 1971; Grew 1980) and granulite xenoliths from kimberlites (Meyer and Brookins 1976; Brookins and Meyer 1974). The only reported occurrence of igneous sapphirine that we have found is from late Archean granitic pegmatites in Enderby Land, Antarctica (Grew 1981). However, the granitic composition of the melt from which this sapphirine crystallized is quite different from the compositions of model mafic melts that crystallize sapphirine in the join anorthite-forsterite-quartz. We have found no descriptions of natural sapphirine in which the occurrence has been attributed to crystallization from a mafic melt, although S.A. Morse (personal communication, 1988) believes that sapphirine in gabbros (hypersthene + plagioclase + magnetite with either sapphirine or spinel) at Wilson Lake, Labrador, Canada, is of igneous origin. Also, sapphirine coexisting with liquid has never been reported in experiments on natural mafic compositions at high pressures. We will first address the apparent discrepancy between our results, which show sapphirine at the liquidus for model mafic compositions, and high pressure crystallization experiments on natural compositions. Then we will discuss the apparent scarcity of natural occurrences of sapphirine crystallized from mafic liquids.

Melting experiments on natural compositions have been carried out on peridotites, primitive basalts, high-alumina basalts and andesites. Figure 2 is not sufficiently complex to model these compositions accurately, but simplified analogs would lie near the base between forsterite and enstatite (peridotite), near piercing point E (basalt), along the line I–J (high-alumina basalt), and near piercing point J (andesite).

We now ask which of these model compositions would show sapphirine coexisting with liquid. Melting and crystallization of model compositions in Fig. 2 cannot be discussed rigorously without reference to quaternary phase relationships, but for present purposes, some qualitative observations are nevertheless useful. Initial melts of the model peridotite would be in equilibrium with pyroxene, spinel, and olivine (point E), and increased amounts of melting would drive the liquid compositions toward the base of the diagram. Thus, sapphirine would not occur. Model high-alumina basalts between I and J, and model andesites at J would crystallize enstatite + anorthite and enstatite + anorthite + quartz, respectively. Again, sapphirine would not occur. Model basalts at E would initially crystallize enstatite and spinel with sapphirine being added at lower temperatures. Thus, sapphirine would occur but only at temperatures well below the liquidus. Although the gap between the model compositions in Fig. 2 and natural compositions is large, the experimental results nevertheless suggest that at 20 kbar sapphirine would be found only in experiments on basalt and only at temperatures well below the liquidus. Sapphirine typically occurs in small amounts and forms very small crystals. Thus, in the presence of large amounts of other phases, as would be the case for experiments well below the liquidus, sapphirine could be missed.

Alternatively, it might be argued that the stability field of natural sapphirine is sufficiently altered by the presence of other components that it would not ever be in equilibrium with natural mafic liquids. Sapphirine produced in our experiments duplicates at least 90% by weight of the composition of natural sapphirine; iron is the only major component of natural sapphirine that is missing. The liquidus stability fields of other relevant minerals (olivine, enstatite, diopside, spinel, plagioclase, garnet) in the system  $\text{CaO} - \text{MgO} - \text{Al}_2\text{O}_3 - \text{SiO}_2$  are shifted by the addition of such components as  $\text{FeO}$ ,  $\text{TiO}_2$ , and  $\text{Na}_2\text{O}$ , but in no case does total elimination of a liquidus stability field occur. Therefore, we argue that sapphirine would crystallize from a basaltic magma cooled at high pressures.

If our evidence for the existence of a liquidus stability field for sapphirine in equilibrium with mafic magmas is accepted, it is necessary to explain the apparent absence of natural occurrences. Three reasons may contribute to this absence. First, crystallization at pressures in the vicinity of 20 kbar may not represent a significant component of the crystallization history of natural basalts. Presnall and Hoover (1987) have argued from phase relationships in the system  $\text{CaO} - \text{MgO} - \text{Al}_2\text{O}_3 - \text{SiO}_2$  that fractional crystallization of mid-ocean ridge

magmas occurs over a range of pressures up to about 11 kbar. Constraints on the existence of fractional crystallization of basalts at higher pressures are weak mainly because of an increasingly deficient knowledge of phase equilibrium relationships as pressure increases, but generalized petrogenetic models have been advanced (for example O'Hara 1965, 1968) that include fractional crystallization at these higher pressures. It is reasonable to suppose that basalts generated at pressures greater than 20 kbar will crystallize at all lower pressures as they pass upward to the earth's surface. Thus, we consider an absence of fractional crystallization near 20 kbar to be possible but unlikely.

Second, if sapphirine does crystallize from basaltic magmas at high pressures, low pressure re-equilibration could remove any remnants of it. Other minerals considered to crystallize from basaltic magmas at high pressures, such as garnet, are not preserved as phenocrysts. Therefore, the absence of sapphirine is not surprising.

Third, some of the occurrences of sapphirine attributed to subsolidus reactions may instead be the result of crystallization directly from a melt. The most interesting candidate for re-evaluation that we have found is a report by Griffin and O'Reilly (1986) of a xenolith from the Delegate breccia pipe, Australia, that contains sapphirine, plagioclase ( $An_{48}$ ), aluminous clinopyroxene, and garnet. They proposed that this unusual assemblage developed by subsolidus reaction from a clinopyroxene + spinel + plagioclase cumulate during cooling from  $>1400^\circ\text{C}$  to  $1000^\circ\text{C}$  at pressures near 15 kbar. Because part of this assemblage (sapphirine + plagioclase) occurs in equilibrium with liquid in Fig. 2, we suggest that the sapphirine-clinopyroxene-garnet-plagioclase assemblage in this xenolith may have crystallized directly from a magma at high pressure.

Another interesting occurrence of sapphirine has been reported from the Beni-Bouchera mafic-ultramafic massif, Morocco (Kornprobst et al. 1982). Kornprobst (1969) proposed that this massif was crystallized initially from a magma at about  $1400^\circ\text{C}$ , 25 kbar, and subsequently recrystallized at  $1100\text{--}1200^\circ\text{C}$ , 15–20 kbar. In the garnet pyroxenites of this complex, sapphirine occurs in coronas that consist of spinel cores encased successively outward by sapphirine, garnet, and clinopyroxene. The sapphirine in these coronas was interpreted by Kornprobst et al. (1982) to be produced during the subsolidus recrystallization at  $1100\text{--}1200^\circ\text{C}$ . In view of the igneous history of the Beni Bouchera complex and the fact that part of the corona assemblage (spinel + sapphirine) can coexist with liquid (see Fig. 2), we believe that an igneous origin for the sapphirine should be considered.

A potentially important aspect of the crystallization of sapphirine from basaltic magmas at high pressures is the partitioning of trace elements between sapphirine and liquid. Partition coefficients are presently unknown, so the effect of sapphirine crystallization on petrogenetic models based on trace element considerations is uncertain.

*Acknowledgements.* This research was supported by National Science Foundation Grant EAR-8418685 to D.C. Presnall. We thank D. Deuring for his assistance in the microprobe analyses.

## References

- Ackermann D, Seifert F, Schreyer W (1975) Instability of sapphirine at high pressures. *Contrib Mineral Petrol* 50:79–92
- Albee AL, Ray L (1970) Correction factors for electron-probe microanalysis of silicates, oxides, carbonates, phosphates and silicates. *Anal Chem* 42:1408–1414
- Andersen O (1915) The system anorthite-forsterite-silica. *Am J Sci* 39:407–454
- Anonymous (1969) The international practical temperature scale of 1968. *Metrologia* 5:35–44
- Boyd FR, England JL (1960) Apparatus for phase equilibrium measurements at pressures up to 50 kilobars and temperatures up to  $1750^\circ\text{C}$ . *J Geophys Res* 65:741–748
- Brookins DG, Meyer HOA (1974) Crustal and upper mantle stratigraphy beneath Kansas. *Geophys Res Lett* 1:269–272
- Dallwitz WB (1968) Co-existing sapphirine and quartz in granulite from Enderby Land, Antarctica. *Nature* 219:476–477
- Chen C-H, Presnall DC (1975) The system  $\text{Mg}_2\text{SiO}_4\text{--SiO}_2$  at pressures up to 25 kilobars. *Am Mineral* 60:398–406
- Clark SP Jr, Schairer JF, De Neufville J (1962) Phase relations in the system  $\text{CaMgSi}_2\text{O}_6\text{--CaAl}_2\text{SiO}_6\text{--SiO}_2$  at low and high pressure. *Carnegie Inst Washington* 61:59–68
- Foster WR (1950a) Synthetic sapphirine and its stability field in the system  $\text{MgO--Al}_2\text{O}_3\text{--SiO}_2$ . *J Am Ceramic Soc* 33:73–84
- Foster WR (1950b) Synthetic sapphirine and its stability field in the system  $\text{MgO--Al}_2\text{O}_3\text{--SiO}_2$ . *J Geol* 58:135–151
- Green TH, Ringwood AE (1967) Crystallization of basalt and andesite under high pressure hydrous conditions. *Earth Planet Sci Lett* 3:481–489
- Grew ES (1980) Sapphirine + quartz association from Archean rocks in Enderby Land, Antarctica. *Am Mineral* 65:821–836
- Grew ES (1981) Surinamite, taaffeite, and beryllian sapphirine from pegmatites in granulite-facies rocks of Casey Bay, Enderby Land, Antarctica. *Am Mineral* 66:1022–1033
- Griffin WL, O'Reilly SY (1986) Mantle-derived sapphirine. *Mineral Mag* 50:635–640
- Irvine TN (1975) Olivine-pyroxene-plagioclase relations in the system  $\text{Mg}_2\text{SiO}_4\text{--CaAl}_2\text{Si}_2\text{O}_8\text{--KAlSi}_3\text{O}_8\text{--SiO}_2$  and their bearing on the differentiation of stratiform intrusions. *Carnegie Inst Washington* 74:492–500
- Keith ML, Schairer JF (1952) The stability field of sapphirine in the system  $\text{MgO--Al}_2\text{O}_3\text{--SiO}_2$ . *J Geol* 60:181–186
- Kornprobst J (1969) Le massif ultrabasique des Beni Bouchera (Rif Interne, Maroc): Etude des péridotites de haute température et de haute pression, et des pyroxenolites à grenat ou sans grenat, qui leur sont associées. *Contrib Mineral Petrol* 23:283–322
- Kornprobst J, Piboule M, Boudeulle M, Roux L (1982) Corundum-bearing garnet pyroxenites at Beni-Bousera (Morocco): an exceptionally Al-rich clinopyroxene from "grosphydites" associated with ultramafic rocks. *Terra Cognita* 2:257–259
- Kushiro I (1968) Compositions of magmas formed by partial zone melting in the earth's upper mantle. *J Geophys Res* 73:619–634
- Kushiro I, Yoder HS Jr (1966) Anorthite-forsterite and anorthite-enstatite reactions and their bearing on the basalt-eclogite transformation. *J Petrol* 7:337–362
- Longhi J (1987) Liquidus equilibria and solid solution in the system  $\text{CaAl}_2\text{Si}_2\text{O}_8\text{--Mg}_2\text{SiO}_4\text{--CaSiO}_3\text{--SiO}_2$  at low pressure. *Am J Sci* 287:265–331
- Meng LK, Moore JM Jr (1972) Sapphirine-bearing rocks from Wilson Lake, Labrador. *Can Mineral* 11:777–790
- Meyer HOA, Brookins DG (1976) Sapphirine, sillimanite and garnet in granulite xenoliths from Stogdale kimberlite, Kansas. *Am Mineral* 61:1194–1202

- Morse SA, Talley JH (1971) Sapphirine reactions in deep-seated granulites near Wilson Lake, Central Labrador, Canada. *Earth Planet Sci Lett* 10:325–328
- O'Hara MJ (1965) Primary magmas and the origin of basalts. *Scott J Geol* 1:19–40
- O'Hara MJ (1968) The bearing of phase equilibria studies in synthetic and natural systems in the origin and evolution of basic and ultrabasic rocks. *Earth Sci Rev* 4:69–133
- O'Hara MJ, Yoder HS Jr (1967) Formation and fractionation of basic magmas at high pressures. *Scott J Geol* 3:67–117
- Presnall DC (1966) The join forsterite-diopside-iron oxide and its bearing on the crystallization of basaltic and ultramafic magmas. *Am J Sci* 264:753–809
- Presnall DC (1976) Alumina content of enstatite as a geobarometer for plagioclase and spinel lherzolites. *Am Mineral* 61:582–588
- Presnall DC, Hoover JD (1987) High pressure phase equilibrium constraints on the origin of mid-ocean ridge basalts. In: Mysen BO (ed) *Magmatic processes: physicochemical principles*. *Geochem Soc Spec Pub* 1:75–89
- Presnall DC, Simmons CL, Porath H (1972) Changes in electrical conductivity of a synthetic basalt during melting. *J Geophys Res* 77:5665–5672
- Presnall DC, Brenner NL, O'Donnell TH (1973) Drift of Pt/Pt10Rh and W3Re/W25Re thermocouples in single stage piston-cylinder apparatus. *Am Mineral* 58:771–777
- Presnall DC, Dixon SA, Dixon JR, O'Donnell TH, Brenner NL, Schrock RL, Dycus DW (1978) Liquidus phase relations on the join diopside-forsterite-anorthite from 1 atm to 20 kbar: their bearing on the generation and crystallization of basaltic magma. *Contrib Mineral Petrol* 66:203–220
- Presnall DC, Dixon JR, O'Donnell TH, Dixon SA (1979) Generation of mid-ocean ridge tholeiites. *J Petrol* 20:3–35
- Sen G, Presnall DC (1984) Liquidus phase relationships on the join anorthite-forsterite-quartz at 10 kbar with applications to basalt petrogenesis. *Contrib Mineral Petrol* 85:404–408
- Stolper E (1980) A phase diagram for mid-ocean ridge basalts: preliminary results and implications for petrogenesis. *Contrib Mineral Petrol* 74:13–27
- Taylor HCJ (1973) Melting relations in the system MgO–Al<sub>2</sub>O<sub>3</sub>–SiO<sub>2</sub> at 15 kb. *Geol Soc Am Bull* 84:1335–1348
- Yoder HS Jr, Tilley CE (1962) Origin of basalt magmas: an experimental study of natural and synthetic rock systems. *J Petrol* 3:342–532

Editorial responsibility: I.S.E. Carmichael